

Stability of U(VI) doped calcium silicate hydrate gel in repository-relevant brines studied by leaching experiments and spectroscopy

Wolter, J.-M.; Schmeide, K.; Weiss, S.; Bok, F.; Brendler, V.; Stumpf, T.;

Originally published:

November 2018

Chemosphere 218(2019), 241-251

DOI: <https://doi.org/10.1016/j.chemosphere.2018.11.074>

Perma-Link to Publication Repository of HZDR:

<https://www.hzdr.de/publications/Publ-27649>

Release of the secondary publication
on the basis of the German Copyright Law § 38 Section 4.

CC BY-NC-ND

**Stability of U(VI) doped calcium silicate hydrate gel in repository-
relevant brines studied by leaching experiments and spectroscopy**

Jan-Martin Wolter^a

Katja Schmeide^{b,*}

Stephan Weiss^c

Frank Bok^d

Vinzenz Brendler^e

Thorsten Stumpf^f

All authors are from the Helmholtz-Zentrum Dresden - Rossendorf, Institute of Resource Ecology,
Bautzner Landstraße 400, 01328 Dresden, Germany

^a j.wolter@hzdr.de

^{b,*} k.schmeide@hzdr.de, + 49 351 260 2436 corresponding author

^c s.weiss@hzdr.de

^d f.bok@hzdr.de

^e v.brendler@hzdr.de

^f t.stumpf@hzdr.de

Keywords: uranium, C-S-H, portlandite, carbonate, ionic strength, TRLFS

Colors should be used for print

Abstract

The stability of calcium silicate hydrate (C-S-H) gel doped with uranium to form calcium uranium silicate hydrate (C-U-S-H) gel was investigated in 2.5 M NaCl, 2.5 M NaCl/0.02 M Na₂SO₄, 2.5 M NaCl/0.02 M NaHCO₃ or 0.02 M NaHCO₃ solutions relevant to the geological disposal of radioactive waste. The C-U-S-H gel samples were synthesized by direct U(VI) incorporation and characterized with time-resolved laser-induced luminescence spectroscopy (TRLFS), infrared (IR) spectroscopy, powder X-ray diffraction (XRD), scanning electron microscopy (SEM), differential scanning calorimetry (DSC), and thermogravimetric analysis (TGA). Time-dependent pH changes as well as the Ca, Si and U release from C-U-S-H gels into the brines, determined by inductively coupled plasma mass spectrometry (ICP-MS), were monitored for three calcium-to-silicon (C/S) ratios (0.99, 1.55 and 2.02) over 32 d. Subsequently, changes of the U(VI) speciation and C-S-H mineralogy caused by leaching were investigated with TRLFS, IR spectroscopy and XRD. Results indicated that composition and pH value of the leaching solution, the presence of portlandite as well as formation and solubility of calcite as secondary phase determine the U(VI) retention by C-S-H gel under high saline and alkaline conditions. At high ionic strengths, the Ca release from C-S-H and secondary phases like calcite is increased. Under hyperalkaline conditions only small amounts of U(VI) were released during leaching. A decrease of the pH due to the additional presence of carbonate was linked with an increased U(VI) release from C-S-H gel leading to the formation of aqueous calcium uranyl carbonate in the supernatant solution.

1. Introduction

The long-term isolation of high-level nuclear waste, such as spent fuels from nuclear power plants, in deep geological formations behind multiple protective barriers is recognized worldwide as preferred strategy to protect humans and environment. In this concept, as part of the geo-engineered barrier cementitious materials in the form of concrete or grout are foreseen to ensure mechanical stability and sealing of disposal tunnels. Moreover, cementitious materials are commonly used for the solidification of low and intermediate level radioactive waste. For a reliable long-term safety

assessment of a nuclear waste repository, it is necessary to identify materials and processes that contribute to the retention of radionuclides potentially released due to water intrusion into a disposal site. In addition, criteria that might lead to a mobilization of radionuclides have to be identified.

The immobilization potential of hardened cement paste (HCP) as well as of C-S-H, as main component of HCP, towards radionuclides such as Cm(III), Th(IV) or U(VI) has been shown in a number of literature studies, e.g. (Pointeau et al., 2004; Stumpf et al., 2004; Wieland et al., 1997). Among the components of spent nuclear fuel 95.5% of the mass is contributed by the uranium isotopes ²³⁵, ²³⁶ and ²³⁸ (OECD, 2006). Their long half-lives and high chemo-toxicity render them important long-term pollutants.

Studies on U-containing HCP showed the presence of uranium in the oxidation state +VI mainly inside the C-S-H gel of HCP (Harfouche et al., 2006; Macé et al., 2013; Wersin et al., 2003; Zhao et al., 2000). The structure of C-S-H gel is similar to a defected 14 Å tobermorite structure, consisting of layered polyhedral CaO planes, silicate chains consisting of pairing and bridging Si tetrahedra called “dreierketten” and interlayers filled with water and Ca²⁺ ions (Richardson, 2008). HCP and C-S-H characteristics, such as layer-to-layer distance, length of silicate chains, and co-presence of portlandite are defined by the molar C/S ratio of the cementitious material, which can exceed 1.7 in freshly hydrated Portland cement and fall below 0.6 in nearly decomposed HCP (Grangeon et al., 2013; Taylor, 1993; Thiery et al., 2013). The highest C/S ratio achieved by exclusively C-S-H in HCP is around 1.7 while further Ca is contributed in the form of portlandite (Ca(OH)₂) (Yu et al., 1999).

Studies of C-U-S-H gel using TRLFS have identified 3 different U(VI) bonding environments: (i) a surface complex, (ii) interlayer incorporation, (iii) a Ca uranate-like surface precipitate (Tits et al. (2011; 2015)). An increase of the U(VI) retention by C-S-H gel with increasing C/S ratio was associated with a U(VI) uptake mechanism that involves Ca from the C-S-H interlayers. Androniuk et al. (2017) combined wet chemistry experiments and molecular dynamics computer simulations to identify the sorption behavior of gluconate and U(VI) on C-S-H gel. The authors identified several sorption sites for U(VI) on the C-S-H surface like mono and bidentate outer-sphere uranyl complexes bound to deprotonated oxygens of bridging Si tetrahedra. Due to a sorption of Ca²⁺ ions on the same sorption sites, a competition between uranyl and Ca²⁺ ions was suggested.

Gaona et al. (2012) developed a geochemical model for the interactions between U(VI) and C-S-H gel based on the results of extended X-ray absorption fine structure (EXAFS) spectroscopy (Harfouche et al., 2006) and TRLFS (Tits et al., 2011; Wieland et al., 2010). The authors confirmed that U(VI) is mainly located in the C-S-H interlayers similar to Ca^{2+} ions. In contrast, the release of U(VI) from HCP is controlled by dissolution and recrystallization of the C-U-S-H gel rather than by surface desorption processes (Tits et al., 2015). It is therefore important to identify factors that will affect the stability of C-U-S-H gel, such as pH, ionic strength and composition of the leaching solution, the formation of secondary phases and how these might incorporate U(VI), as well as the U(VI) species and their mobility in the leaching solution.

The majority of investigations on radionuclide retention by cementitious materials, however, have only been performed at low ionic strengths, e.g. (Gaona et al., 2012; Harfouche et al., 2006; Tits et al., 2011). Studies of cementitious materials in high ionic strength solutions include Hill et al. (2006), Kienzler et al. (2010; 2016) and Bube et al. (2014). Hill et al. (2006) studied the dissolution of radionuclide-free C-S-H gel (C/S 0.8–2.0) in 0.1 to 1 M NaCl solutions. The authors found an increasing amount of leached Ca^{2+} with increasing NaCl concentration which was attributed to an ion exchange mechanism between Na and Ca. Kienzler et al. (2010; 2016) and Bube et al. (2014) studied the corrosion of U(VI)-containing cement monoliths in saturated NaCl- or MgCl_2 -rich brines. Comprehensive analyses of drill core fragments and bulk powder samples after long-term leaching showed the presence of a uranophane-like $(\text{Ca}(\text{UO}_2)_2(\text{SiO}_3\text{OH})_2 \cdot 5\text{H}_2\text{O})$ phase while no becquerelite, meta-schoepite or di-uranate phases were detected. The U(VI) concentrations measured in leaching solutions were up to 5×10^{-7} M while a diffusive penetration of halite into the cement monolith surface up to 5 cm was observed.

Carbonate-containing high saline host rock pore waters, containing up to 4 M Na^+ , 2.8 M Cl^- , 0.1 M SO_4^{2-} , and 0.06 M HCO_3^- , are reported for potential sites for nuclear waste repositories, e.g., for Cretaceous argillites in North Germany (Peryt et al., 2010; Wolfgramm et al., 2011), as well as for sedimentary bedrocks in Japan (Hama et al., 2007) and in Canada (Mazurek, 2004). However, to the best of the author's knowledge, systematic studies on the stability of cementitious phases and their

retention potential for U(VI) in complex repository-relevant brines have not been reported in the literature.

Such high ionic strengths pore waters could modify dissolution/recrystallization processes of C-S-H gel including the formation of secondary phases, which in turn could affect the stability of C-S-H gel as well as the U(VI) release or retention.

Thus, the objective of the present work was to evaluate the stability of C-U-S-H gel and its U(VI) retention capability in high ionic strengths pore waters. For this, C-U-S-H gel samples with three different C/S ratios (2.02, 1.55 and 0.99, representing a portlandite saturated C-S-H system as well as chemically degraded cement paste) were prepared and leached in solutions containing 2.5 M NaCl, 0.02 M Na₂SO₄ and/or 0.02 M NaHCO₃. In addition, spectroscopic, microscopic and diffraction techniques were applied before and after leaching to obtain a mechanistic understanding of the underlying processes such as the evolution of the C-S-H gel and of U(VI) species on the solid phase as well as secondary phase formation and formation of U(VI) species in the leaching solution.

2. Materials and experimental methods

2.1. Materials

The synthesis of C-U-S-H gel and subsequent leaching experiments were performed in an inert gas glove box (N₂ atmosphere, O₂ < 2 ppm) using degassed deionized water (18 MΩ cm; mod. Milli-RO/Milli-Q-System, Millipore, Schwalbach, Germany). Prior to experiments, centrifuge tubes (polypropylene, Greiner bio-one, Kremsmünster, Austria) were immersed in 0.1 M HCl for 12 h and subsequently rinsed with deionized water to remove contaminants.

Solid UO₃ was prepared from uranyl peroxide (Chemapol Ltd, Czech Republic) after a method reported by Rosenheim and Daehr (1929). For C-S-H synthesis, KOH (ACS reagent, Roth, Karlsruhe, Germany), NaOH (p. a., Roth), fumed silica (AEROSIL 300, Evonik, Essen, Germany), and carbonate-free CaO (anhydrous, trace metals basis, Sigma-Aldrich, St. Louis, Missouri, USA) were used. Previously, NaOH and KOH surface carbonate was removed by washing the NaOH and KOH pellets several times with degassed deionized water in a Büchner funnel under inert gas atmosphere.

Total inorganic carbonate concentrations of prepared NaOH and KOH solutions were determined with a multi-N/C 2100 S (Analytik Jena, Jena, Germany) and were below 100 μM . For drying, wet C-S-H samples were either frozen in liquid nitrogen, and dried at 1 mbar and $-40\text{ }^{\circ}\text{C}$ for 1 d in a freeze-drying system (mod. ALPHA 1-4 LSCplus, Christ, Osterode am Harz, Germany) or exposed to a CO_2 -free N_2 atmosphere over two weeks.

2.2. Synthesis of C-U-S-H gel

2.2.1. Direct synthesis of C-U-S-H gel

C-U-S-H gel samples (A–C) were prepared applying a direct incorporation method. For this, a U(VI)-containing artificial cement pore water (ACW; (Berner, 1992)) was prepared by adding an excess of solid UO_3 to a solution of 0.18 M KOH and 0.114 M NaOH (pH 13.3) and stirring for a week. Subsequently, the ACW was separated from remaining solid UO_3 by centrifugation ($6800\times g$, mod. Avanti J-20 XP, Beckman Coulter, Krefeld, Germany) and analyzed for U(VI) by ICP-MS analysis (KED-mode, He gas, mod. NexION 350X/Elan 9000, PerkinElmer, Waltham, MA, USA) after adjusting the pH to 2 with concentrated HNO_3 . The resulting ACW contained 19.5 μM U. This U(VI)-containing ACW was added to a mixture of fumed silica and carbonate-free CaO. While the CaO to SiO_2 ratio was varied depending on the targeted C/S ratio (1.0, 1.6, 2.0), the solid-to-liquid (S/L) ratio was fixed at 24 g L^{-1} . Suspensions were shaken end-over-end with a rotator SB2 (Stuart, Staffordshire, UK) for 14 d, and then filtered through a Whatman ashless 541-grade filter (22 μm cut-off). The C-U-S-H gel samples were washed with deionized water and stored moist in sealed tubes for leaching experiments (cf. section 2.3) or dried for spectroscopy. For the determination of the elemental compositions, C-S-H samples were decomposed in hydrofluoric acid and then analyzed for Ca, Si, Na, K, and U by ICP-MS. An additional C-S-H gel (sample J) was synthesized at a S/L ratio of 24 g L^{-1} in U(VI)-free ACW for SEM investigations that required a U(VI)-free C-S-H gel.

2.2.2. Sorption of U(VI) onto C-S-H gel

For a comparison of samples A–C with C-U-S-H gel synthesized by Tits et al. (2011), a further C-U-S-H gel (CSH_{Nitrate}) with a target C/S ratio of 1.3 was prepared using the method proposed by these authors. For this, sample J was exposed to a UO₂(NO₃)₂ solution which contained 19.5 μM U(VI) for 14 d (S/L ratio: 24 g L⁻¹, pH after 14 d: 11.7). Subsequently, the C-U-S-H gel was similarly filtered off, washed with deionized water, and stored moist.

2.3. Leaching experiments

For batch leaching experiments, wet C-U-S-H gel samples (A–C), prepared by direct synthesis, were equilibrated in 2.5 M NaCl, 2.5 M NaCl/0.02 M Na₂SO₄, 2.5 M NaCl/0.02 M NaHCO₃ or 0.02 M NaHCO₃ at a S/L ratio of 10 g L⁻¹ by shaking the samples end-over-end with a rotator SB2 for up to 32 d. Subsequently, the water contents of samples A–C were determined by TGA to determine the actual S/L ratios in each leaching experiment. After different time intervals, up to 768 h, samples were centrifuged at 6800×g. Each supernatant solution was analyzed for Ca, Si and U as well as for the pH value. Solid and liquid phases after leaching were characterized by spectroscopic and further analytical methods (cf. section 2.4.). All leaching experiments mentioned above were performed as triplicates.

Additionally, sample B was leached in 2.5 M NaCl/0.075 M NaHCO₃ for 768 h to visualize changes in the TRLFS spectrum of C-U-S-H gel after leaching in solutions with high concentrations of carbonate. To determine the influence of increasing carbonate concentrations on the pH evolution and U(VI) release from C-U-S-H gel, sample A was exposed to solutions containing 1, 2, 10, 20, 50, and 75 mM NaHCO₃ for 768 h. Subsequently, the supernatants were separated by centrifugation and analyzed for the pH value and released U. To get detailed information about the Ca and Si release in dependence on NaCl concentrations, sample J was exposed to solutions containing 0, 0.5, 1.0, 1.5, 2.0, and 2.5 M NaCl at an actual S/L ratio of 1.5 g L⁻¹ for 7 d. Subsequently, the supernatants were analyzed for Ca and Si.

2.4. Analytical techniques and calculation methods

For TRLFS investigations, C-U-S-H gel samples were suspended in deionized water, transferred into Boro 5.1 (ASTM type 1 class B glass, 5 mm) tubes (Deutero, Kastellaun, Germany) and shock-frozen in liquid N₂. The tubes were placed in a cryogenic cooling system (mod. TG-KKK, KGW-Isotherm, Karlsruhe, Germany) and further cooled with N₂ vapor to a constant temperature of (153 ± 2) K. The cooling of the samples was necessary to generate a detectable U(VI) luminescence signal by the suppression of dynamic quenching effects (Wang et al., 2005a). The laser set-up was optimized for high intensities and good signal-to-noise ratios of the spectra: front entrance of 500 µm, gate width of 2 ms and a delay time between 0.1 µs and 2 ms. To generate the excitation wavelength of 266 nm, a Nd:YAG laser (mod. Minilite, Continuum, Santa Clara, CA, USA) with an average pulse energy of 0.3 mJ was used. Emission wavelengths were detected between 14,947 cm⁻¹ (669 nm) and 27,100 cm⁻¹ (369 nm) by accumulating 100 laser pulses with a spectrograph (mod. iHR 550, HORIBA Jobin Yvon, Unterhaching, Germany) and an ICCD camera (mod. ICCD-3000, HORIBA Jobin Yvon). Positions of luminescence bands were determined by calculating the minima of the second derivative.

Immediately after removing the C-U-S-H gel from the N₂ atmosphere, IR samples were prepared under ambient conditions by mixing approximately 1 mg of the dried samples with 300 mg dried KBr and subsequently pressing for 2 min at 1×10⁹ Pa until clear pellets were obtained. IR samples were measured with a Vertex 70/v spectrometer (Bruker, Billerica, Massachusetts, USA) equipped with a D-LaTGS-detector (Lalanine doped triglycine sulfate), over a range of 400 to 4,000 cm⁻¹ in the transmittance mode, with a spectral resolution of 4 cm⁻¹. Each spectrum was averaged over 64 scans.

Powder XRD data of C-U-S-H gel were collected with a MiniFlex 600 diffractometer (Rigaku, Tokyo, Japan) equipped with a Cu K α X-ray source (40 keV/15 mA) and the D/teX Ultra 1D silicon strip detector. The diffractograms were recorded in the Bragg-Brentano θ -2 θ geometry at a scanning speed of 0.6° per min. For sample preparation, the C-U-S-H gel was mounted as wet paste on a zero-background Si sample holder with a Kapton window under inert gas conditions. The subsequent Rietveld analysis of diffractograms was done with the program PDXL 2 (Rigaku) and the ICDD PDF-4+ 2016 database.

For TGA and DSC investigations, the various C-S-H gels (sample J (freeze-dried), samples A–C (wet pastes), sample C (dried under N₂ atmosphere)) were transferred in an Al₂O₃ crucible and measured between 25 and 1000 °C at 20 K min^{−1} in an Ar atmosphere with a STA 449 F5 Jupiter thermal analysis instrument (Netzsch, Selb, Germany).

SEM imaging with secondary electrons was performed using a S-4800 microscope (Hitachi, Tokyo, Japan) operated at an accelerating voltage of 10 kV. For sample preparation, the freeze-dried C-S-H gel was put onto an aluminum stub covered with a carbon tab.

The pH values of solutions were measured with a pH meter (inoLab pH 720, WTW, Weilheim, Germany) with a SenTix[®] Mic pH microelectrode (WTW) calibrated against standard pH buffers (pH: 6.865, 9.180 and 12.454) (WTW). The pH values of solutions with high ionic strengths were corrected using a method reported by Altmaier et al. (2003; 2008).

The solubilities of calcite in 0–2.75 M NaCl solutions at pH 10, of portlandite in 0–3.2 M NaCl solutions and of a C-S-H gel (C/S 1.1) in 0–3.2 M NaCl solutions at a S/L ratio of 1.5 g L^{−1} were calculated with the geochemical speciation code Geochemist's Workbench (GWB), Module React (vers. 11.0.6) (Bethke, 2008) using the Pitzer ion interaction model. The thermodynamic database was "THEREDA" (Thermodynamic Reference Database, <https://www.thereda.de>, Release No. 6). U(VI) speciation in the carbonate-containing supernatant solution was also calculated with GWB using the "PSI/Nagra Chemical Thermodynamic Database 12/07" (Thoenen et al., 2014). The parameter files used for solubility and speciation calculations are added as supplementary material.

3. Results and discussion

3.1. Characterization of C-U-S-H gel

3.1.1. Elemental composition

C-U-S-H gel samples A–C, synthesized by the direct incorporation method, possessed C/S ratios of 0.99, 1.55 and 2.02 (Table 1). From the Ca and Si amounts applied for C-S-H synthesis, ≤2.3% remained in the ACW after the reaction time of 14 d (Table S1). That means, the C/S ratios after syntheses are almost identical to the targeted C/S ratios. More than 96.5% of U, originally present in

the alkaline starting solution, was taken up by the C-S-H samples. U(VI) loadings were between 1.34×10^{-4} and $2.29 \times 10^{-4} \text{ mol kg}^{-1}$ which correspond to 31.9 to 54.5 ppm U(VI). The distribution ratios, $R_d = \frac{c_0 - c_{eq}}{c_{eq}} \cdot \frac{V}{m} [\text{L kg}^{-1}]$, increased from 1.2×10^3 to $1.2 \times 10^4 \text{ L kg}^{-1}$ with increasing C/S ratio.

Compared to the distribution ratios reported by Tits et al. (2011) (1.0×10^3 to $1.0 \times 10^6 \text{ L kg}^{-1}$), Pointeau et al. (2004) (3×10^4 to $1.5 \times 10^5 \text{ L kg}^{-1}$) as well as determined for $\text{CSH}_{\text{Nitrate}}$ ($2.1 \times 10^3 \text{ L kg}^{-1}$), the direct incorporation method provides comparable R_d values. While the sample $\text{CSH}_{\text{Nitrate}}$ possesses a high U(VI) loading, its R_d value is similar to those of samples A–C. This is caused by a hydration effect and discussed in the supplementary material (Text S2).

Table 1
Composition of C-U-S-H gel samples and distribution ratios (R_d) for U uptake by C-S-H gel.

Sample	C/S ratio	Ca [mol-%]	Si [mol-%]	Na [mol-%]	K [mol-%]	U [ppm]	R_d [L kg^{-1}]
C	2.02	63.3	31.4	2.2	3.1	54.5	11700
B	1.55	53.6	34.5	4.9	6.8	37.3	4820
A	0.99	37.9	38.3	9.4	14.4	31.9	1169
J	1.35	53.7	39.9	2.9	3.6	<0.01	–
$\text{CSH}_{\text{Nitrate}}$	1.25	54.3	43.6	0.7	1.4	183	2130

3.1.2. IR spectroscopic, powder XRD, TGA and DSC investigations

Analyses of the samples A–C by IR (Fig. S2, Text S3), XRD (Fig. S3, Text S4), TGA and DSC (Fig. S4, Text S5) were entirely consistent with the formation of a tobermorite-like C-S-H gel with the co-existence of 18 mass-% portlandite for sample C (Text S1). Water contents of samples A–C were between 77 and 88% as shown in Table S2, Fig. S1 and Text S1.

3.1.3. TRLFS investigations

The TRLFS spectra and luminescence properties of the C-U-S-H gel samples are compiled in Fig. 1 and Table S3, respectively. The first emission band in the TRLFS spectra of C-U-S-H is termed 0-0

band and originates from the de-excitation of the $5f_{\delta}$ und $5f_{\phi}$ atomic orbital of U(VI) to the vibration ground state of the σ_u molecular orbital, mainly dominated by axial bound O (Su et al., 2014). Further de-excitations to vibration coupled states of σ_u are termed 0-1, 0-2 and so on.

A shift of emission bands towards lower energies (red-shift) was reported in the literature for an increase of electron density of the uranyl ligands (Liu and Beitz, 2006; Tits et al., 2011). This can be caused by a ligand change from e.g. water against hydroxide ions in ACW or a sorption of U(VI) on the C-S-H surface whereby hydroxide ligands are substituted against silicate. An incorporation of uranyl in the C-S-H interlayer should even further red-shift the emission bands due to the complete absence of hydroxide ligands and the exclusive presence of silicate ligands in the C-S-H interlayer. The electron density from relevant ligands increases in the following order: $\text{H}_2\text{O} < \text{OH}^- < \text{SiO}_4^{4-}$.

Observed luminescence emission bands of U(VI) dissolved in ACW (Fig. 1) are in good agreement with bands reported for the uranyl hydroxide complex, $\text{UO}_2(\text{OH})_4^{2-}$, occurring in ACW under comparable conditions (Tits et al., 2011) (Table S3). The 0-0 band of sample C is located at $19,992 \text{ cm}^{-1}$, thus between the 0-0 bands of the U(VI)/C-S-H surface complex ($20,150 \text{ cm}^{-1}$) and the U(VI)/C-S-H incorporated species ($19,844 \text{ cm}^{-1}$), reported by Tits et al. (2011) for a C-U-S-H gel with a C/S ratio of 1.07. Compared to the further emission lines of samples A–C, the 0-0 band is weakly pronounced. Since the 0-0 band is located in higher proximity to the 0-0 band of U(VI) coordinated by hydroxide in ACW, it is concluded that the 0-0 band in samples A–C and $\text{CSH}_{\text{Nitrate}}$ is mainly caused by a U(VI) species located on the C-S-H surface where OH^- and SiO_4^{4-} ligands are present.

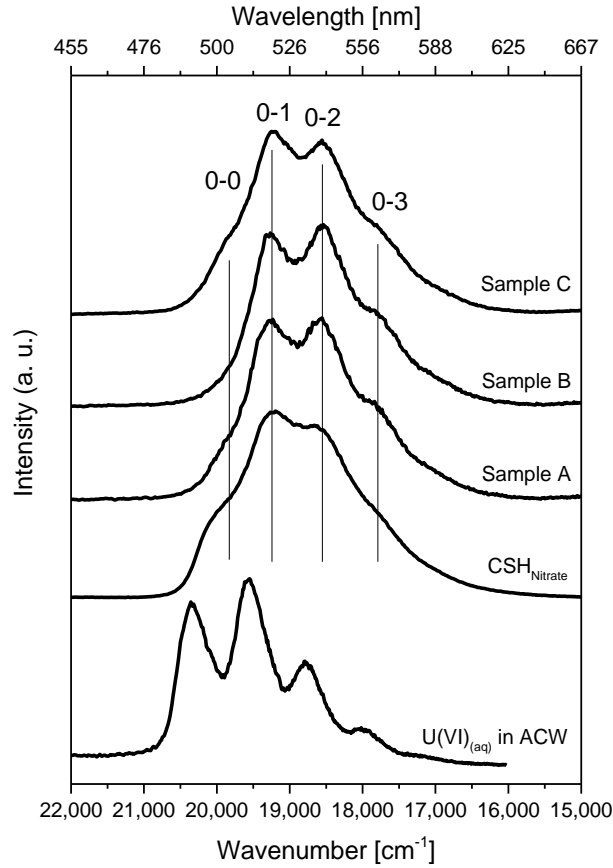


Fig. 1. TRLFS spectra of samples C, B, A and $\text{CSH}_{\text{Nitrate}}$ (C/S: 2.02, 1.55, 0.99 and 1.25) before leaching as well as $\text{U(VI)}_{\text{(aq)}}$ (19.5 μM) in ACW.

Note that the 0-0 band of the reference sample $\text{CSH}_{\text{Nitrate}}$, synthesized according to the procedure reported by Tits et al. (2011), is more distinct than in samples A–C. Due to the surface exposure of sample J to uranyl nitrate during the synthesis of $\text{CSH}_{\text{Nitrate}}$, U(VI) is probably first sorbed on the C-S-H surface before it is incorporated in the C-S-H interlayer by recrystallization. This was also described by Tits et al. (2011) who observed an ongoing incorporation of U(VI) in the C-S-H crystal structure over a time period of 6 months after U(VI) surface sorption on C-S-H gel. Due to the shorter synthesis time of 14 d compared to 6 months, $\text{CSH}_{\text{Nitrate}}$ probably possesses a higher amount of surface sorbed U(VI) which is also higher compared to samples A–C where U(VI) is mainly located in the C-S-H interlayers.

The positions of the 0-1 and 0-2 bands of samples A–C are distinct around 19,300 and 18,500 cm^{-1} , respectively, and most probably belong to uranyl incorporated in the C-S-H interlayer. Thus, during the 14 d of synthesis of the C-U-S-H gel the direct incorporation method ensures a fast

incorporation of U(VI) in the C-S-H gel whereas the U(VI) sorption procedure requires longer time periods (up to 6 months) to acquire a high ratio of U(VI) incorporated in the C-S-H interlayer. Thus, for the preparation of C-U-S-H gel, representative for cement encapsulated nuclear waste, within short times (14 d) the direct incorporation method is preferable.

Luminescence decay lifetime analyses of samples A–C show the presence of two U(VI) species, one with short lifetimes of 103–119 μs and one with long lifetimes of 521–604 μs (Table S3). These lifetimes are in the same range as the lifetimes determined for the U(VI)/C-S-H surface complex ((205–293) \pm 50 μs) and the U(VI)/C-S-H incorporated species ((546–647) \pm 50 μs) reported by Tits et al. (2011). However, it should be noted that the lifetime of U(VI) species in solid C-S-H gel is influenced by sample preparation, C/S ratio, moisture of the sample, and presence of quenchers. Thus, a species identification based on the lifetime is only reasonable to a limited extent (Chisholm-Brause et al., 2001; 2004).

From the TRIFS study it can be concluded that the U(VI) in samples A–C is predominantly incorporated into the interlayer structure of C-S-H gel and to a much smaller degree sorbed on the C-S-H gel surface.

3.2. Leaching of C-U-S-H gel

The results of batch leaching experiments, between 18 and 768 h exposure time, are shown for sample B (C/S 1.55) in terms of Ca, Si and U release into the supernatant solution (Fig. 2[a], Fig. S5, Fig. S6). The actual S/L ratios during leaching, that differed from the applied S/L ratio of 10 g L⁻¹ due to the bulk water content of the wet gels, were determined with 1.2, 1.5 and 2.3 g L⁻¹ for samples A, B and C, respectively (Table S2).

For all samples (A–C), final Ca, Si and U concentrations as well as pH values of the supernatant solutions after 768 h leaching are given in Table 2. Between 18 and 768 h leaching, the pH values varied with \pm 0.1 around the values given in Table 2. For the calculation of the percentage dissolution of samples A–C, the Ca, Si and U concentrations for a hypothetical complete dissolution at actual S/L ratios are given in Table S4.

3.2.1. Leaching in 2.5 M NaCl and 2.5 M NaCl/0.02 M Na₂SO₄

The contact of samples A–C with a 2.5 M NaCl leaching solution leads to a Ca concentration in solution of about 1.0–6.6 mM (Fig. 2, Table 2). Consequently, the pH value of the leaching solution increased from 7 to 11.7–12.2.

Hill et al. (2006), who monitored the Ca release from radionuclide-free C-S-H gel into 0 to 1 M NaCl solutions over 1 month (Table S5 ([Ca]: 2–29 mM leached, C/S: 1.0–2.0, S/L: 10–77 g L⁻¹), showed that the presence of 1 M NaCl increased the amount of Ca leached from C-S-H gel compared to pure water. The authors suggested an ion exchange mechanism between Na and Ca which increased the Ca release from C-S-H gel in the presence of 1 M NaCl. They also found a good agreement of the Ca release from portlandite and C-S-H gel with a high C/S ratio in 1 M NaCl.

Compared to this study, the results of the present study show a lower Ca mobilization into solution which is attributed to the lower S/L ratios (1.2 to 2.3 g L⁻¹) and salting in/salting out effects that have an impact on the Ca solubility. To study the C-S-H gel solubility behavior at low S/L ratios, sample J (C/S 1.35) was exposed to salt solutions between 0 and 2.5 M NaCl at a S/L ratio of 1.5 g L⁻¹ over 7 d. Between 0 and 1.5 M NaCl, an increase of the Ca release from 1.1 mM towards 2.7 mM (Fig. 2[b]) was observed. At higher NaCl concentrations, the Ca release stagnated around 2.7 mM. The Si release of sample J reached a maximum of 0.95 mM between 0.5 and 1 M NaCl (Fig. S7). Leaching results of samples A–C in pure water were in good agreement with these observations and showed a lower release of Ca, especially for C-S-H gel with a low C/S ratio, compared to the leaching in 2.5 M NaCl (Fig. 2[b]). Additionally, the Ca release from a C-S-H gel with a C/S ratio of 1.1 was calculated at a S/L ratio of 1.5 g L⁻¹ for 0 to 3.2 M NaCl solutions (Fig. 2[b]). The calculations showed an increase of the Ca release from the C-S-H gel up to a maximum at 1.5 M NaCl and a slight decrease at higher NaCl concentrations. This is in good agreement with the leaching results of samples B and J. Therefore, in terms of Ca release from C-S-H gel the effect of a 2.5 M NaCl solution is comparable to a 1 M NaCl solution.

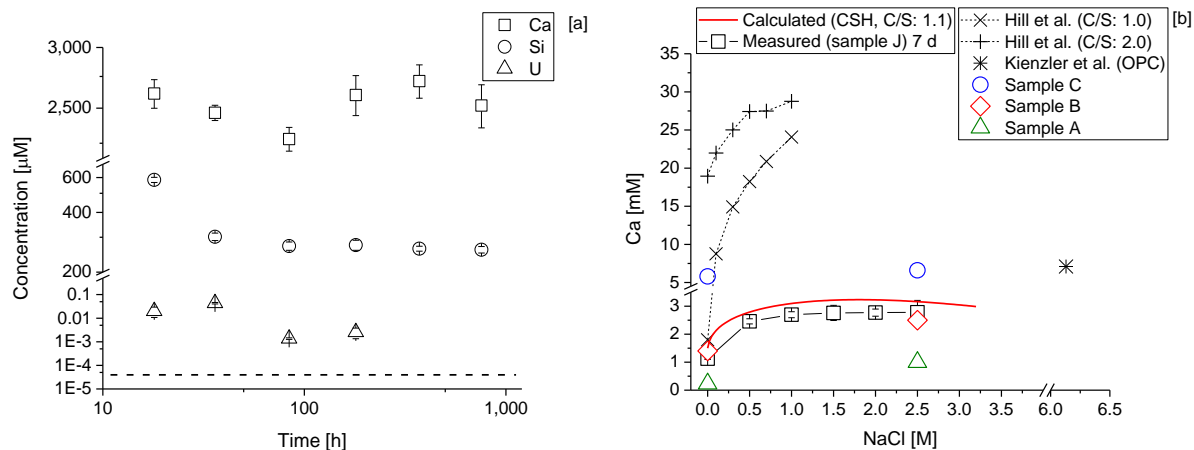


Fig. 2. Calcium, silicon and uranium concentration in the supernatant solution after leaching of sample B in 2.5 M NaCl as a function of time (ICP-MS detection limit for U is $4.2 \times 10^{-5} \mu\text{M}$ (dashed line)) [a]. Calculated solubility of a C-S-H gel with a C/S ratio of 1.1 in NaCl solutions between 0 and 3.2 M at a S/L ratio of 1.5 g L^{-1} [b] (calculation cf. section 2.4). Measured calcium release from sample J (S/L 1.5 g L^{-1}) between 0 and 2.5 M NaCl and from samples C (S/L 2.3 g L^{-1}), B (S/L 1.5 g L^{-1}) and A (S/L 1.2 g L^{-1}) in water and 2.5 M NaCl in comparison to literature data of Hill et al. (2006) (S/L 50 g L^{-1}) and Kienzler et al. (2010) (OPC = ordinary Portland cement) [b].

The Si release of sample B into the 2.5 M NaCl solution amounts to 2.1% of total Si (0.26 mM) after 768 h (Fig. 2[a]). Please note that due to the release of Ca and Si from the C-S-H gel, the final C/S ratios of the C-S-H gel samples after leaching are decreased in dependency on the initial C/S ratios and the composition of the leaching solutions (Table 2). To ease the recognition of the various samples, however, we continue to use the C/S before leaching in the following text. Generally, an increased Ca and Si release from concrete at higher ionic strength is equivalent to a faster chemical degradation of HCP in a nuclear waste repository.

Table 2

Calcium, silicon and uranium concentrations and pH values of supernatant solutions as well as C/S ratios determined after 768 h leaching of sample C (C/S 2.02, S/L 2.3 g L⁻¹), sample B (C/S 1.55, S/L 1.5 g L⁻¹) and sample A (C/S 0.99, S/L 1.2 g L⁻¹). Values in brackets give the percentage dissolution of the ions present in the respective samples.

	Leaching solutions				
	Water	2.5 M NaCl	2.5 M NaCl/ 0.02 M Na ₂ SO ₄	2.5 M NaCl/ 0.02 M NaHCO ₃	0.02 M NaHCO ₃
Ca [mM]					
Sample C	5.8 (13.0)	6.6 (14.8)	7.4 (16.6)	0.21 (0.5)	0.034 (0.1)
Sample B	1.4 (7.5)	2.5 (13.4)	2.4 (12.8)	0.16 (0.9)	0.062 (0.3)
Sample A	0.23 (2.4)	1.0 (10.3)	1.9 (19.6)	0.18 (1.9)	0.17 (1.8)
Si [mM]					
Sample C	0.029 (0.1)	0.11 (0.5)	0.068 (0.3)	3.8 (17.1)	5.3 (23.9)
Sample B	0.13 (1.1)	0.26 (2.1)	0.26 (2.1)	2.4 (19.8)	8.4 (69.4)
Sample A	0.48 (4.9)	0.64 (6.5)	0.48 (4.9)	2.6 (26.5)	8.6 (87.8)
U [μM]					
Sample C	7.8×10 ⁻⁴	< 4.2×10 ⁻⁵	< 4.2×10 ⁻⁵	0.16 (4.6)	0.022 (0.6)
Sample B	8.7×10 ⁻⁴	< 4.2×10 ⁻⁵	< 4.2×10 ⁻⁵	0.20 (12.5)	0.64 (40.0)
Sample A	1.1×10 ⁻³	< 4.2×10 ⁻⁵	< 4.2×10 ⁻⁵	0.18(16.4)	0.24 (21.8)
pH					
Sample C	12.0	12.2	12.0	10.4	10.3
Sample B	11.7	11.9	11.7	10.1	9.6
Sample A	11.4	11.7	11.5	9.9	9.3
C/S ratio after leaching					
Sample C	1.75	1.57	1.69	—	—
Sample B	1.45	1.37	1.38	—	—
Sample A	1.01	0.96	0.84	—	—

Only 2.7% (4.3×10^{-2} μM) of the total U(VI) of sample B was released in the first 36 h of leaching (Fig. 2[a]). After 186 h, the U(VI) concentration decreased below the ICP-MS detection limit of 4.2×10^{-5} μM, indicating a reincorporation of U(VI) into the C-S-H gel or into a secondary phase formed.

Kienzler et al. (2016) investigated the U(VI) release from U(VI)-containing cementitious material prisms submerged in highly saline salt solutions (5.98 M NaCl, 0.02 M CaSO₄, 0.02 M MgSO₄) over 32 years and observed an increase of uranium concentrations from $2 \times 10^{-3} \mu\text{M}$ towards $5 \times 10^{-1} \mu\text{M}$ over that time period. Despite the differences in solution composition, mineral assemblages and S/L ratios, both experiments showed only small amounts of mobilized uranium due to the presence of saline solutions.

To clarify the U(VI) speciation for the leached solids in the present study, TRLFS was applied (Fig. 3). The spectrum of sample B leached in 2.5 M NaCl is broadened and shifted towards higher energies indicating the presence of a uranophane-like phase with a maximum around $19,230 \text{ cm}^{-1}$ (Fig. 3). The presence of a diuranate-type U(VI) mineral would shift the maximum of the spectrum towards lower energies around $18,100 \text{ cm}^{-1}$ (Tits et al., 2011) and was therefore excluded.

These findings correspond well with the observations of Kienzler et al. (2010) who characterized concrete drill dust after leaching by XRD, TRLFS and EXAFS and reported the presence of a uranophane-like phase.

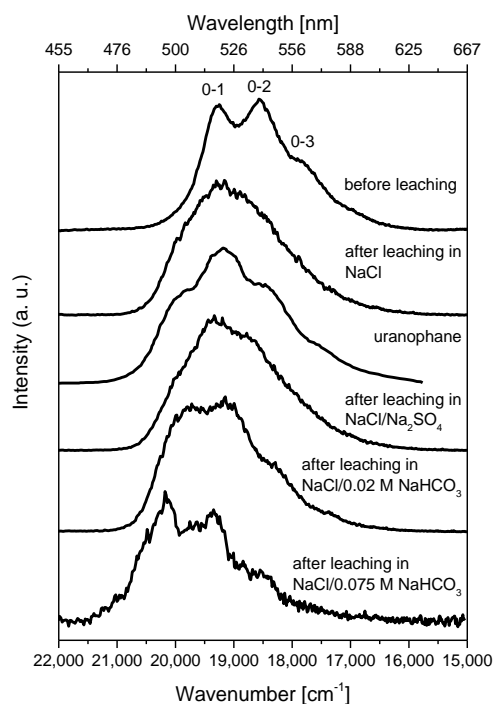
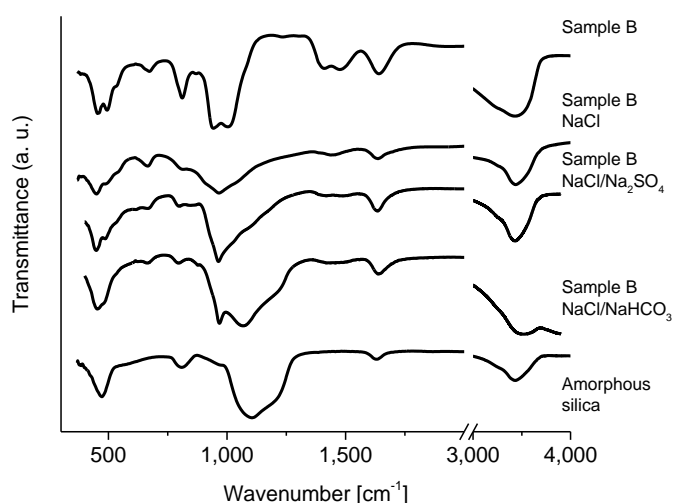


Fig. 3. TRLFS spectra of sample B (C/S 1.55) before and after 768 h of contact with different leaching solutions (2.5 M NaCl, 2.5 M NaCl/0.02 M Na₂SO₄, 2.5 M NaCl/0.02 M NaHCO₃, 2.5 M NaCl/0.075 M NaHCO₃) in comparison to the spectrum of uranophane (Kienzler et al., 2010).

396

397 The IR spectrum of sample B leached in 2.5 M NaCl shows a decrease of band resolution due to a
 398 reduction of the C/S ratio and crystallinity due to leaching (Fig. 4). The Si–OH vibration at 960 cm^{-1}
 399 was not shifted which indicates that the silanol (Si–OH) groups with bridging tetrahedra of the C-S-H
 400 structure remained intact after leaching in 2.5 M NaCl.

401



402

403 **Fig. 4.** IR spectra of sample B (C/S 1.55) before and after 768 h of contact with different leaching solutions (2.5 M NaCl,
 404 2.5 M NaCl/0.02 M Na_2SO_4 , 2.5 M NaCl/0.02 M NaHCO_3) in comparison to the spectrum of amorphous silica
 405 (AEROSIL 300).
 406

407 In summary, due to increased ionic strength (2.5 M NaCl) the Ca and Si release from C-S-H gel
 408 increased compared to pure water while the U(VI) environment partially changed from C-S-H towards
 409 a uranophane-like phase. Nonetheless, the structure of the C-S-H gel remained mostly stable and
 410 almost no U(VI) was released into the aqueous phase.

411 With regard to safety assessment of HCP barriers in deep geological waste disposals for actinides,
 412 after contact with about 2.5 M NaCl solutions, a uranophane-like phase becomes the mobility
 413 controlling phase for U(VI) on the HCP surface.

414 The Ca, Si and U release of sample B in 2.5 M NaCl/0.02 M Na_2SO_4 after 768 h (Fig. S5) was
 415 similar to the Ca, Si and U release in 2.5 M NaCl (Table 2). Moreover, TRLFS and IR investigations
 416 of C-U-S-H gel leached in 2.5 M NaCl/0.02 M Na_2SO_4 show no further changes compared to the
 417 leaching in 2.5 M NaCl (Fig. 3, Fig. 4). Only the Si release kinetic in the first 18 h of leaching is

decreased due to the additional presence of 0.02 M Na_2SO_4 (Fig. 2[a], Fig. S5). This could be caused by the adsorption of sulfate on the C-S-H surface as reported by (Divet and Randriambololona, 1998). After 768 h of leaching, the Si concentrations in both leaching experiments matched. Conclusively, 0.02 M Na_2SO_4 does not have any negative effects on C-S-H stability or U(VI) retention by C-S-H gel.

3.2.2. Leaching in 2.5 M NaCl/0.02 M NaHCO_3 and 0.02 M NaHCO_3

The presence of carbonate increased the amount of leached Si for samples A–C to 17.1–26.5% (2.4–3.8 mM) in 2.5 M NaCl/0.02 M NaHCO_3 and to 23.9–87.8% (5.3–8.6 mM) in 0.02 M NaHCO_3 (Fig. S6, Table 2, Fig. 5). Thus, for all samples a partial destabilization of the silicate chains of the C-S-H structure leading to the formation of $\text{SiO}_{2(\text{am})}$ can be assumed. This was confirmed by IR spectroscopy due to the appearance of a shoulder at $1,234\text{ cm}^{-1}$ which is also present in the IR spectrum of $\text{SiO}_{2(\text{am})}$ (Fig. 4). For sample C leached in carbonate-containing solutions, the $\text{SiO}_{2(\text{am})}$ band was only weakly pronounced (Fig. S8), suggesting that a part of the NaHCO_3 preferentially reacted with portlandite, consequently, less $\text{SiO}_{2(\text{am})}$ was formed. However, the IR spectrum of sample C leached in 2.5 M NaCl/0.02 M NaHCO_3 shows a distinct carbonate band around $1,400\text{ cm}^{-1}$ (Fig. S8) that probably belongs to calcite (Sato and Matsuda, 1969) formed by reaction of portlandite and carbonate. In contrast, only a weak carbonate band around $1,400\text{ cm}^{-1}$ is observed in the IR spectrum of sample B leached in 2.5 M NaCl/0.02 M NaHCO_3 , indicating a low amount of solid CaCO_3 . This implies that, compared to $\text{Ca}(\text{OH})_2$, the C-S-H gel reacts to a lesser extent with carbonate.

Compared to carbonate-free leaching experiments, the leaching of sample B in 2.5 M NaCl/0.02 M NaHCO_3 causes a lower Ca concentration (0.9%, 0.16 mM) as well as a lower pH (10.1) in the leaching solution (Table 2, Fig. 5). Under carbonate-free conditions, the pH in a concrete system is buffered by the dissolution of portlandite. In the presence of HCO_3^- , the precipitation of CaCO_3 removes Ca^{2+} and OH^- from the solution, thus, lowering the pH and Ca concentrations compared to carbonate-free solutions. Final C/S ratios of leached samples were not determined since the Ca content of C-U-S-H gel after leaching is distributed between C-S-H and CaCO_3 .

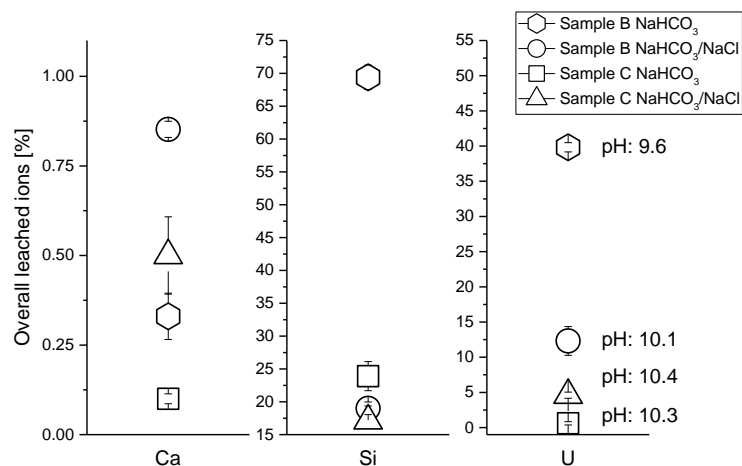


Fig. 5. Percentage amount of leached calcium, silicon and uranium with corresponding pH values after leaching of sample B (C/S 1.55) and sample C (C/S 2.02) in 0.02 M NaHCO₃ or 2.5 M NaCl/0.02 M NaHCO₃ for 768 h.

Before leaching, the SEM image shows the typical C-S-H fiber structure (Ashraf and Olek, 2016) (Fig. 6[a]). After leaching in 0.02 M NaHCO₃, the overgrowth of the C-S-H surface of sample J with euhedral calcite crystals (Ashraf and Olek, 2016) was observed (Fig. 6[b]).

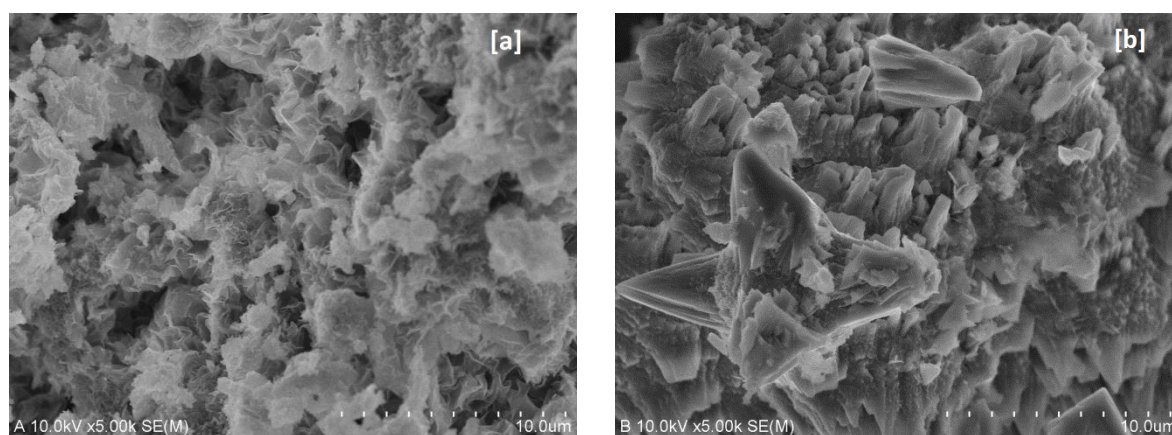


Fig. 6. SEM images of sample J (C/S 1.35) before leaching [a] and after leaching in 0.02 M NaHCO₃ [b].

The U(VI) release of sample B due to leaching in 2.5 M NaCl/0.02 M NaHCO₃ is strongly increased to 12.5% (0.2 μM, pH 10.1) of the overall U(VI) (circle in Fig. 5, Table 2). This effect is even more distinct in the absence of 2.5 M NaCl where the 0.02 M NaHCO₃ leaching solution mobilizes 40% of the U(VI) of sample B (hexagon in Fig. 5, Table 2). In contrast, sample C shows a lower amount of released U(VI) of 4.6% (0.16 μM, pH 10.4) in 2.5 M NaCl/0.02 M NaHCO₃ and

0.6% in 0.02 M NaHCO₃ (triangle/square in Fig. 5, Table 2). These results are a clear indication for an increased U(VI) mobility in the presence of carbonate and a reduction of the pH which influences the U(VI) speciation in the leaching solution.

Under hyperalkaline (pH > 12) conditions, U(VI) hydroxide complexes such as UO₂(OH)₄²⁻ or UO₂(OH)₃⁻ dominate U(VI) speciation and solubility (Torrents, 2014), whereas a lower pH (8 < pH < 10.6) soluble uranyl carbonate complexes (e.g., UO₂(CO₃)₃⁴⁻) can occur in carbonate-containing aqueous systems (Wang et al., 2004). In the presence of 0.034-0.21 mM Ca, determined in solution in the current study, ternary calcium uranyl carbonate complexes, Ca₂UO₂(CO₃)₃(aq) and CaUO₂(CO₃)₃²⁻, would likely form (Bernhard et al., 2001). These ternary species impede the U(VI) sorption onto solids as shown, for instance, for ferrihydrite and quartz (Fox et al., 2006), clay (Joseph et al., 2013) and granite (Schmeide et al., 2014).

To investigate U(VI) speciation changes in the leaching solution from UO₂(OH)₄²⁻ or UO₂(OH)₃⁻ towards aqueous calcium uranyl tricarboxylate in dependence on pH and amount of NaHCO₃, a leaching series of sample A in solutions containing up to 75 mM NaHCO₃ was performed (Fig. 7[a]). The leaching solutions of sample A show a non-linear decrease of the pH value coupled with increasing amounts of released U in dependence on the NaHCO₃ contents. TRLFS investigations confirmed the predominance of aqueous calcium uranyl tricarboxylate (Fig. 7[b]) for NaHCO₃ concentrations ≥ 75 mM which corresponds to pH 9.3. This complex possessed well-defined emission bands at 20,803, 19,964, 19,157 and 18,348 cm⁻¹ and a lifetime of 750 μs (at 153 K) similar to the data reported by Wang et al. (2004) (20,812, 19,952, 19,131 and 18,315 cm⁻¹; 1282 μs (at 6 K)) (Table S2). This complex was also observed in the presence of 2.5 M NaCl when the pH and carbonate content were similar (Fig. 7[b]).

Speciation calculations performed for the composition determined in the supernatant solution of sample B after leaching in 2.5 M NaCl/0.02 M NaHCO₃ ([Ca]: 0.159 mM, [Si]: 2.4 mM, [U]: 0.2 μM, [carbonate]: 14 mM, pH: 10.1), supported the formation of aqueous calcium uranyl tricarboxylate complexes.

At higher pH values, the high concentration of OH^- suppresses the formation of calcium uranyl tricarbonatate, and spectra with low intensities and without any band resolution are detected (sample C sup. sol. NaHCO_3 , Fig. 7[b]).

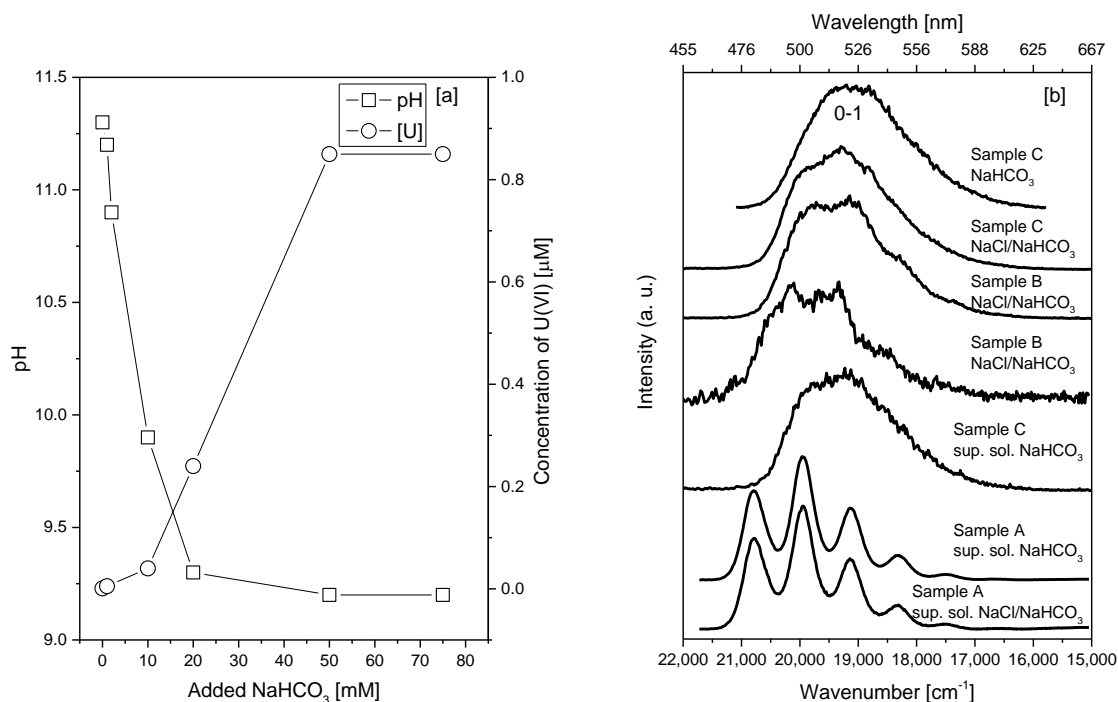


Fig. 7. Evolution of pH value and U concentration of the supernatant solution of sample A as function of added NaHCO_3 , (768 h leaching, S/L 1.2 g L^{-1}) [a]. TRLFS spectra of sample C leached in 0.02 M NaHCO_3 , sample C leached in $2.5 \text{ M NaCl}/0.02 \text{ M NaHCO}_3$, sample B leached in $2.5 \text{ M NaCl}/0.02 \text{ M NaHCO}_3$, sample B leached in $2.5 \text{ M NaCl}/0.075 \text{ M NaHCO}_3$, supernatant solution of sample C leached in 0.02 M NaHCO_3 , supernatant solution of sample A leached in 0.1 M NaHCO_3 , supernatant solution of sample A leached in $2.5 \text{ M NaCl}/0.075 \text{ M NaHCO}_3$, (768 h leaching) [b].

Nonetheless, further factors such as formation of secondary CaCO_3 phases like calcite, vaterite and aragonite and their solubility in dependence on ionic strength may also influence the U(VI) mobility due to sorption of U(VI) on these CaCO_3 polymorphs. To investigate the influence of the secondary phase formation, TRLFS spectra of leached samples A–C were recorded. The TRLFS spectra of sample B leached in $2.5 \text{ M NaCl}/0.02 \text{ M NaHCO}_3$ or $2.5 \text{ M NaCl}/0.075 \text{ M NaHCO}_3$ (Fig. 7[b]) show a shift of the 0-1 band towards higher energies from $19,318 \text{ cm}^{-1}$ to $19,980 \text{ cm}^{-1}$ and $20,234 \text{ cm}^{-1}$, respectively. These shifts towards higher energies can be explained by an increased amount of U(VI) sorbed or incorporated in calcite formed as secondary phase as reported in the literature (Elzinga et al., 2004; Geipel et al., 1997; Smith et al., 2015).

TRLFS investigations of a natural U(VI)-containing calcite showed 0-0 and 0-1 bands at 20,790 and 20,000 cm^{-1} , respectively (Wang et al., 2005b). Since the leached samples contain a mixture of U(VI) sorbed on calcite and U(VI) remaining in the C-S-H gel, the recorded spectra after leaching in carbonate-containing solutions are caused by an overlap of both U(VI) coordination environments.

Rietveld analyses of the XRD patterns of sample C and A leached in 2.5 M NaCl/0.02 M NaHCO_3 (Fig. 8) show, that C-U-S-H gel and portlandite are partly converted to CaCO_3 whereby exclusively calcite was detected.

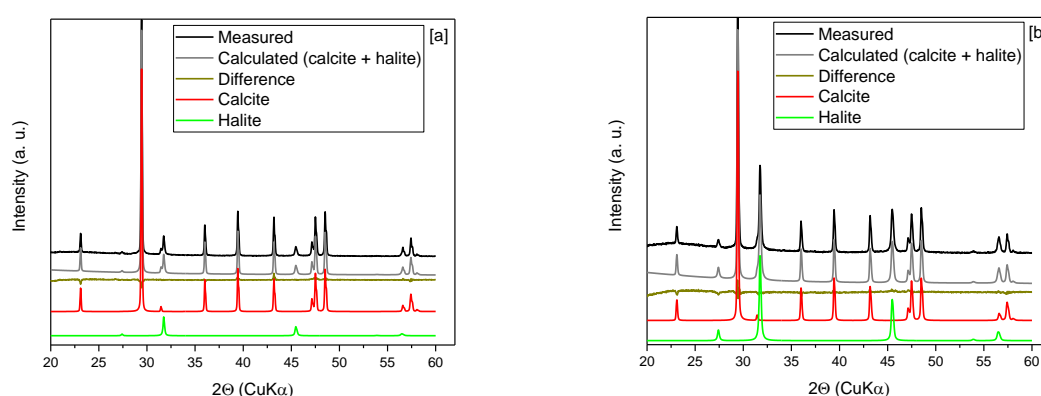


Fig. 8. Powder XRD patterns of samples C (C/S 2.02) [a] and A (C/S 0.99) [b] after leaching in 2.5 M NaCl/0.02 M NaHCO_3 , (768 h leaching), calcite (database card number 01-083-4601), halite (database card number 00-005-0628), (Cu K α X-ray source).

XRD patterns of samples C and A leached in 0.02 M NaHCO_3 but absence of NaCl (Fig. S9) also suggest that the samples are partly converted into secondary CaCO_3 phases: A part of sample A is converted into 70% calcite and 30% metastable aragonite while sample C, that consists of C-U-S-H gel and portlandite, is partly converted into 80% calcite and 20% metastable vaterite (Table S6). A comparison with data from (Black et al., 2007), who investigated carbonation effects in mechanochemically prepared C-S-H gels with C/S ratios between 0.2 and 1.5 under ambient conditions, revealed the occurrence of predominantly vaterite for samples with C/S ratios ≥ 0.67 while in C-S-H samples with C/S ratios ≤ 0.5 mainly aragonite was detected. Although this trend is similar to that of the present study, the absence of calcite and the lower C/S boundary for the vaterite formation confirm differences between both studies. This can probably be attributed to different preparation methods and carbonation techniques of both studies. Further studies where similar cementitious systems were exposed to carbonate detected either the simultaneous presence of calcite, vaterite and

aragonite (Chang and Fang, 2015; Ibanez et al., 2007) or a reversed trend where aragonite was observed at higher and vaterite at lower C/S ratios (Auroy et al. (2018)). These findings suggest that the formation of the various CaCO_3 modifications depends on the cement system and the carbonation method. The results of the present study also suggest that high amounts of NaCl suppress the formation of metastable CaCO_3 modifications such as vaterite and aragonite. This is tentatively attributed to an increased recrystallization rate of these phases as suggested by Takita et al. (2007).

TRLFS investigations of sample C leached in exclusively 0.02 M NaHCO_3 showed a broad spectrum without any band resolution that is less blue-shifted than the spectrum of sample B leached in 0.02 M NaHCO_3 (Fig. 7[b]). Due to the higher amount of portlandite in sample C, combined with the higher solubility of portlandite compared to C-S-H gel, most of the carbonate is precipitated as calcite and vaterite (Fig. S9). Thus, the amount of carbonate in solution, which could contribute to a decomposition of the C-U-S-H structure, is reduced. Simultaneously, a higher pH value in solution after CaCO_3 precipitation is maintained. Since portlandite does not contain U(VI) its dissolution does not contribute to a U(VI) mobilization. Calcite, however, acts as a U(VI) sink as implied by the TRLFS investigations (Fig. 7[b]). Compared to metastable CaCO_3 phases like vaterite, better U(VI) retention properties were reported for calcite (Noubactep et al., 2006).

Compared to the leaching of sample C in 0.02 M NaHCO_3 solution, the additional presence of 2.5 M NaCl increased the amounts of released U(VI) and Ca from 0.6 to 4.6% and from 0.1 to 0.5%, respectively (square/triangle, Fig. 5), although the pH values were with 10.3 and 10.4 very similar. Solubility calculations (cf. section 2.4) showed that the calcite solubility increases with increasing NaCl concentrations between 0 and 2.5 M NaCl (Fig. 9[a]). Also the solubility of portlandite increases between 0 and 1 M NaCl, but decreases afterwards (Fig. 9[b]). If, in turn, less calcite precipitates, which also leads to somewhat higher Ca^{2+} and CO_3^{2-} concentrations in the supernatant, less U(VI) can be immobilized on the calcite surface. Thus, the formation of aqueous calcium uranyl tricarboxylate is favored against the formation of U(VI) hydroxide complexes at a pH around 10.4.

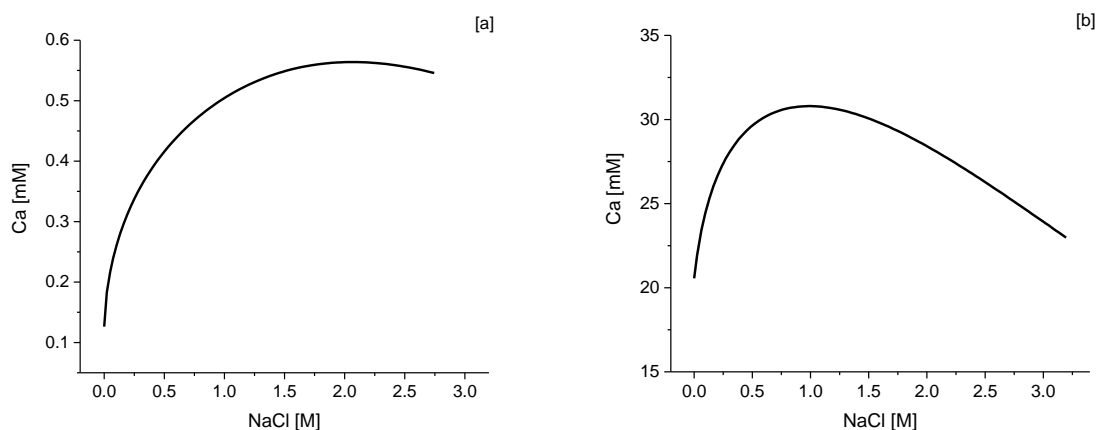


Fig. 9. Calculated solubilities of calcite in 0–2.75 M NaCl solutions at pH 10 [a] and of portlandite in 0–3.2 M NaCl solutions [b]. Details of calculations are given in section 2.4.

4. Conclusions

The stability of C-U-S-H gel and its U(VI) retention capability in high ionic strengths pore waters was studied. For this, C-U-S-H gel samples with three different C/S ratios (0.99, 1.55 and 2.02) were synthesized applying a direct incorporation method which ensured an U(VI) incorporation predominantly into the interlayer structure of C-S-H.

These C-U-S-H gel samples were leached in solutions containing 2.5 M NaCl, 0.02 M Na₂SO₄ and/or 0.02 M NaHCO₃, thus, reflecting conditions expected for host rock pore waters of potential nuclear waste repositories. The results showed that the composition of the leaching solution had a direct influence on the alteration of the C-S-H structure and evolution of the pH value in these systems.

Compared to pure water, the leaching in a 2.5 M NaCl solution increased the release of Ca from C-S-H gel from 1.4 to 2.5 mM (initial C/S ratio: 1.55, S/L ratio: 1.5 g L⁻¹). The effect of a 2.5 M NaCl solution was comparable to a 1 M NaCl solution. Despite the release of Ca, IR investigations suggested that the C-U-S-H structure remained stable, while U(VI) retention was largely unaffected due to a formed uranophane-like phase detected by TRLFS. The additional presence of 0.02 M Na₂SO₄ did not show any effect on the stability of the C-U-S-H structure.

In the presence of carbonate (0.02 M), the U(VI) retention was coupled to the alteration stage of the C-S-H structure as well as to the pH evolution of the leaching solution. Carbonate preferentially reacted with portlandite to form calcite and vaterite while the C-U-S-H structure remained intact, which was confirmed by XRD and IR investigations. Furthermore, the absence of a distinct blue-shift of the U(VI) luminescence spectrum of the leached portlandite-rich sample confirmed the persistent presence of U(VI) in the C-U-S-H gel. In the case of C-U-S-H gel with a lower C/S ratio, representing altered concrete, carbonate removed Ca from solution which subsequently led to a further release of Ca from the C-U-S-H gel. Thus, the polyhedral CaO plane of the C-U-S-H structure was increasingly destabilized, as verified by the appearance of Si-O bands of amorphous silica in the IR spectrum. The thereby formed secondary CaCO_3 phases, detected by XRD after leaching, contributed to a certain extent to U(VI) retention, as shown by a blue-shift of the U(VI) luminescence spectrum of the leached solid. Nevertheless, the destabilization of the polyhedral CaO plane of the C-U-S-H structure led to an enhanced release of U(VI). Due to an overall lower pH value in the presence of carbonate, aqueous calcium uranyl tricarbonate was formed as confirmed by TRLFS.

The U(VI) release from the portlandite-rich C-U-S-H sample into carbonate-containing solutions was slightly higher in the presence than in the absence of NaCl. This was attributed to an increased calcite solubility at enhanced salinities, which led to higher Ca^{2+} and CO_3^{2-} concentrations in solution, and thus, to formation of aqueous calcium uranyl tricarbonate.

In the context of a nuclear waste repository, the high immobilization potential of C-U-S-H gel for U(VI) appears to be unaffected by highly saline groundwaters. In the presence of carbonate, however, it is expected that the release of U(VI) from C-U-S-H gel will be greatly enhanced.

Acknowledgements

The German Federal Ministry for Economic Affairs and Energy (BMWi) is thanked for financial support (no. 02 E 11415B). The authors would like to thank Dr. Harald Foerstendorf (HZDR), Dr. Gerhard Geipel (HZDR), Dr. Atsushi Ikeda-Ohno (HZDR), Dr. Jan Tits (PSI) and Dr. Barbara Lothenbach (Empa) for the helpful discussions and advice as well as K. Heim, S. Beutner, B. Pfützner

and A. Scholz (all from HZDR) for IR, ICP-MS and SEM measurements. Furthermore, the authors would like to specifically thank the two anonymous reviewers for their valuable comments.

Appendix A. Supplementary material

Supplementary data associated with this article can be found, in the online version, at

References

- Altmaier, M., Metz, V., Neck, V., Müller, R., Fanghänel, T., 2003. Solid-liquid equilibria of $\text{Mg}(\text{OH})_2(\text{cr})$ and $\text{Mg}_2(\text{OH})_3\text{Cl} \cdot 4 \text{H}_2\text{O}(\text{cr})$ in the system $\text{Mg-Na-H-OH-O-Cl-H}_2\text{O}$ at 25 °C. *Geochim Cosmochim Acta* 67, 3595-3601.
- Altmaier, M., Neck, V., Fanghänel, T., 2008. Solubility of Zr(IV), Th(IV) and Pu(IV) hydrous oxides in CaCl_2 solutions and the formation of ternary Ca-M(IV)-OH complexes. *Radiochim Acta* 96, 541-550.
- Androniuk, I., Landesman, C., Henocq, P., Kalinichev, A., 2017. Adsorption of gluconate and uranyl on C-S-H phases: Combination of wet chemistry experiments and molecular dynamics simulations for the binary systems. *Phys Chem Earth* 99, 194-203.
- Ashraf, W., Olek, J., 2016. Carbonation behavior of hydraulic and non-hydraulic calcium silicates: potential of utilizing low-lime calcium silicates in cement-based materials. *J Mater Sci* 51, 6173-6191.
- Auroy, M., Poyet, S., Le Bescop, P., Torrenti, J.-M., Charpentier, T., 2018. Comparison between natural and accelerated carbonation (3% CO_2): Impact on mineralogy, microstructure, water retention and cracking. *Cement Concrete Res* 109, 64-80.
- Berner, U.R., 1992. Evolution of pore water chemistry during degradation of cement in a radioactive waste repository environment. *Waste Manage* 12, 201-219.
- Bernhard, G., Geipel, G., Reich, T., Brendler, V., Amayri, S., Nitsche, H., 2001. Uranyl(VI) carbonate complex formation: Validation of the $\text{Ca}_2\text{UO}_2(\text{CO}_3)_{(3)(\text{aq})}$ species. *Radiochim Acta* 89, 511-518.
- Bethke, C., 2008. *Geochemical and Biogeochemical Reaction Modeling*. Cambridge University Press, pp. 565.
- Black, L., Breen, C., Yarwood, J., Garbev, K., Stemmermann, P., Gasharova, B., 2007. Structural features of C-S-H(I) and its carbonation in air - A Raman spectroscopic study. Part II: Carbonated phases. *J Am Ceram Soc* 90, 908-917.
- Bube, C., Metz, V., Schild, D., Rothe, J., Dardenne, K., Lagos, M., Plaschke, M., Kienzler, B., 2014. Combining thermodynamic simulations, element and surface analytics to study U(VI) retention in corroded cement monoliths upon > 20 years of leaching. *Phys Chem Earth* 70-71, 53-59.
- Chang, J., Fang, Y., 2015. Quantitative analysis of accelerated carbonation products of the synthetic calcium silicate hydrate(C-S-H) by QXRD and TG/MS. *J. Therm. Anal. Calorim.* 119, 57-62.
- Chisholm-Brause, C.J., Berg, J.M., Little, K.M., Matzner, R.A., Morris, D.E., 2004. Uranyl sorption by smectites: spectroscopic assessment of thermodynamic modeling. *J Colloid Interf Sci* 277, 366-382.
- Chisholm-Brause, C.J., Berg, J.M., Matzner, R.A., Morris, D.E., 2001. Uranium(VI) sorption complexes on montmorillonite as a function of solution chemistry. *J Colloid Interf Sci* 233, 38-49.
- Divet, L., Randriambololona, R., 1998. Delayed ettringite formation: The effect of temperature and basicity on the interaction of sulphate and C-S-H phase. *Cement Concrete Res* 28, 357-363.

647 Elzinga, E.J., Tait, C.D., Reeder, R.J., Rector, K.D., Donohoe, R.J., Morris, D.E., 2004. Spectroscopic
648 investigation of U(VI) sorption at the calcite-water interface. *Geochim Cosmochim Acta* 68, 2437-
649 2448.

650 Fox, P.M., Davis, J.A., Zachara, J.M., 2006. The effect of calcium on aqueous uranium(VI) speciation
651 and adsorption to ferrihydrite and quartz. *Geochim Cosmochim Acta* 70, 1379-1387.

652 Gaona, X., Kulik, D.A., Macé, N., Wieland, E., 2012. Aqueous-solid solution thermodynamic model
653 of U(VI) uptake in C-S-H phases. *Appl Geochem* 27, 81-95.

654 Geipel, G., Reich, T., Brendler, V., Bernhard, G., Nitsche, H., 1997. Laser and X-ray spectroscopic
655 studies of uranium-calcite interface phenomena. *J Nucl Mater* 248, 408-411.

656 Grangeon, S., Claret, F., Linard, Y., Chiaberge, C., 2013. X-ray diffraction: a powerful tool to probe
657 and understand the structure of nanocrystalline calcium silicate hydrates. *Acta Crystallogr B* 69, 465-
658 473.

659 Hama, K., Kunimaru, T., Metcalfe, R., Martin, A.J., 2007. The hydrogeochemistry of argillaceous
660 rock formations at the Horonobe URL site, Japan. *Phys Chem Earth* 32, 170-180.

661 Harfouche, M., Wieland, E., Dähn, R., Fujita, T., Tits, J., Kunz, D., Tsukamoto, M., 2006. EXAFS
662 study of U(VI) uptake by calcium silicate hydrates. *J Colloid Interf Sci* 303, 195-204.

663 Hill, J., Harris, A.W., Manning, M., Chambers, A., Swanton, S.W., 2006. The effect of sodium
664 chloride on the dissolution of calcium silicate hydrate gels. *Waste Manage* 26, 758-768.

665 Ibanez, J., Artus, L., Cusco, R., Lopez, A., Menendez, E., 2007. Hydration and carbonation of
666 monoclinic C₂S and C₃S studied by Raman spectroscopy. *J. Raman Spectrosc.* 38, 61-67.

667 Joseph, C., Stockmann, M., Schmeide, K., Sachs, S., Brendler, V., Bernhard, G., 2013. Sorption of
668 U(VI) onto Opalinus Clay: Effects of pH and humic acid. *Appl Geochem* 36, 104-117.

669 Kienzler, B., Borkel, C., Metz, V., Schlieker, M., 2016. Long-Term Interactions of Full-Scale
670 Cemented Waste Simulates with Salt Brines. *Karlsruher Institut für Technologie (KIT) Report Nr.*
671 7721.

672 Kienzler, B., Metz, V., Brendebach, B., Finck, N., Plaschke, M., Rabung, T., Rothe, J., Schild, D.,
673 2010. Chemical status of U(VI) in cemented waste forms under saline conditions. *Radiochim Acta* 98,
674 675-684.

675 Liu, G.K., Beitz, J.V., 2006. The Chemistry of the Actinide and Transactinide Elements. in: Morss,
676 L.R., Edelstein, N.M., Fuger, J. (Eds.). Springer, Dordrecht, The Netherlands.

677 Macé, N., Wieland, E., Dähn, R., Tits, J., Scheinost, A.C., 2013. EXAFS investigation on U(VI)
678 immobilization in hardened cement paste: influence of experimental conditions on speciation.
679 *Radiochim Acta* 101, 379-389.

680 Mazurek, M., 2004. Long-term Used Nuclear Fuel Waste Management – Geoscientific Review of the
681 Sedimentary Sequence in Southern Ontario. Institute of Geological Sciences, University of Bern,
682 Bern, Switzerland.

683 Noubactep, C., Sonnefeld, J., Merten, D., Heinrichs, T., Sauter, M., 2006. Effects of the presence of
684 pyrite and carbonate minerals on the kinetics of the uranium release from a natural rock. *J Radioanal*
685 *Nucl Chem* 270, 325-333.

686 OECD, 2006. Physics and Safety of Transmutation Systems: A Status Report. OECD Papers, 2 rue
687 Andre Pascal, 75775 Paris Cedex 16.

688 Peryt, T.M., Geluk, M.C., Mathiesen, A., Paul, J., Smith, K., 2010. Zechstein. in: Doornenbal, J.C.,
689 Stevenson, A.G. (Eds.). *Petroleum Geological Atlas of the Southern Permian Basin Area*. EAGE
690 Publications b.v., Houten, the Netherlands.

691 Pointeau, I., Landesman, C., Giffaut, E., Reiller, P., 2004. Reproducibility of the uptake of U(VI) onto
692 degraded cement pastes and calcium silicate hydrate phases. *Radiochim Acta* 92, 645-650.

693 Richardson, I.G., 2008. The calcium silicate hydrates. *Cement Concrete Res* 38, 137-158.

694 Rosenheim, A., Daehr, H., 1929. Uranium tetroxide-hydrate. *Z Anorg Allg Chem* 181, 177-182.

695 Sato, M., Matsuda, S., 1969. Structure of vaterite and infrared spectra. *Z Kristallogr Krist* 129, 405-
696 410.

697 Schmeide, K., Gürtler, S., Müller, K., Steudtner, R., Joseph, C., Bok, F., Brendler, V., 2014.
698 Interaction of U(VI) with Äspö diorite: A batch and in situ ATR FT-IR sorption study. *Appl Geochem*
699 49, 116-125.

700 Smith, K.F., Bryan, N.D., Swinburne, A.N., Bots, P., Shaw, S., Natrajan, L.S., Mosselmans, J.F.W.,
701 Livens, F.R., Morris, K., 2015. U(VI) behaviour in hyperalkaline calcite systems. *Geochim*
702 *Cosmochim Acta* 148, 343-359.

703 Stumpf, T., Tits, J., Walther, C., Wieland, E., Fanghänel, T., 2004. Uptake of trivalent actinides
704 (curium(III)) by hardened cement paste: a time-resolved laser fluorescence spectroscopy study. *J*
705 *Colloid Interf Sci* 276, 118-124.

706 Su, J., Wang, Z.M., Pan, D.Q., Li, J., 2014. Excited states and luminescent properties of UO_2F_2 and its
707 solvated complexes in aqueous solution. *Inorg Chem* 53, 7340-7350.

708 Takita, Y., Eto, M., Sugihara, H., Nagaoka, K., 2007. Promotion mechanism of co-existing NaCl in
709 the synthesis of CaCO_3 . *Mater Lett* 61, 3083-3085.

710 Taylor, H.F.W., 1993. Nanostructure of C-S-H - Current Status. *Adv Cem Based Mater* 1, 38-46.

711 Thiery, M., Dangla, P., Belin, P., Habert, G., Roussel, N., 2013. Carbonation kinetics of a bed of
712 recycled concrete aggregates: A laboratory study on model materials. *Cement Concrete Res* 46, 50-65.

713 Thoenen, T., Hummel, W., Berner, U., Curti, E., 2014. The PSI/Nagra Chemical Thermodynamic
714 Database 12/07.

715 Tits, J., Geipel, G., Macé, N., Eilzer, M., Wieland, E., 2011. Determination of uranium(VI) sorbed
716 species in calcium silicate hydrate phases: A laser-induced luminescence spectroscopy and batch
717 sorption study. *J Colloid Interf Sci* 359, 248-256.

718 Tits, J., Walther, C., Stumpf, T., Macé, N., Wieland, E., 2015. A luminescence line-narrowing
719 spectroscopic study of the uranium(VI) interaction with cementitious materials and titanium dioxide.
720 *Dalton Trans* 44, 966-976.

721 Torrents, A.M., 2014. Doctoral Thesis: Effect of Alkaline Conditions on Near-field Processes of a
722 Spent Nuclear Fuel Geological Repository. Department of Chemical Engineering. Universitat
723 Politècnica de Catalunya-Barcelona Tech, Catalunya.

724 Wang, Z.M., Zachara, J.M., Gassman, P.L., Liu, C.X., Qafoku, O., Yantasee, W., Catalano, J.G.,
725 2005a. Fluorescence spectroscopy of U(VI)-silicates and U(VI)-contaminated Hanford sediment.
726 *Geochim Cosmochim Acta* 69, 1391-1403.

727 Wang, Z.M., Zachara, J.M., McKinley, J.P., Smith, S.C., 2005b. Cryogenic laser induced U(VI)
728 fluorescence studies of a U(VI) substituted natural calcite: Implications to U(VI) speciation in
729 contaminated Hanford sediments. *Environ Sci Technol* 39, 2651-2659.

730 Wang, Z.M., Zachara, J.M., Yantasee, W., Gassman, P.L., Liu, C.X., Joly, A.G., 2004. Cryogenic
731 laser induced fluorescence characterization of U(VI) in Hanford vadose zone pore waters. *Environ Sci*
732 *Technol* 38, 5591-5597.

733 Wersin, P., Johnson, L.H., Schwyn, B., Berner, U., Curti, E., 2003. Redox Conditions in the Near-field
734 of a Repository for SF/HLW and ILW in Opalinus Clay. Nagra Technical Report NTB 02-13. Nagra,
735 Wettingen, Switzerland.

736 Wieland, E., Macé, N., Dähn, R., Kunz, D., Tits, J., 2010. Macro- and micro-scale studies on U(VI)
737 immobilization in hardened cement paste. *J Radioanal Nucl Chem* 286, 793-800.

738 Wieland, E., Tits, J., Spieler, P., Dobler, J.P., 1997. Interaction of Eu(III) and Th(IV) with sulphate-
739 resisting Portland cement. *Materials Research Society Symposium Proceedings*, pp. [d]573-578.

- 740 Wolfgramm, M., Thorwart, K., Rauppach, K., Brandes, J., 2011. Zusammensetzung, Herkunft und
741 Genese geothermaler Tiefengrundwässer im Norddeutschen Becken (NDB) und deren Relevanz für
742 die geothermische Nutzung. Z. geol. Wiss. 39, 173-193.
- 743 Yu, P., Kirkpatrick, R.J., Poe, B., McMillan, P.F., Cong, X.D., 1999. Structure of calcium silicate
744 hydrate (C-S-H): Near-, mid-, and far-infrared spectroscopy. J Am Ceram Soc 82, 742-748.
- 745 Zhao, P., Allen, P.G., Sylwester, E.R., Viani, B.E., 2000. The partitioning of uranium and neptunium
746 onto hydrothermally altered concrete. Radiochim Acta 88, 729-736.
- 747